THE JOURNAL OF BIOLOGICAL CHEMISTRY VOL. 282, NO. 40, pp. 29701–29711, October 5, 2007

Regulation of Mesodermal Differentiation of Mouse Embryonic Stem Cells by Basement Membranes*[S]

Received for publication, December 14, 2006, and in revised form, August 3, 2007 Published, JBC Papers in Press, August 9, 2007, DOI 10.1074/jbc.M611452200

Hironobu Fujiwara[‡§], Yoshitaka Hayashi[§1], Noriko Sanzen[‡§], Reiko Kobayashi[‡], Charles N. Weber[§], Tomomi Emoto[§], Sugiko Futaki[‡§], Hitoshi Niwa[¶], Patricia Murray[‖], David Edgar[**], and Kiyotoshi Sekiguchi[‡§2]

*From the [‡]Institute for Protein Research, Osaka University, Osaka 565-0871, Japan, the [§]Sekiguchi Biomatrix Signaling Project, Exploratory Research for Advanced Technology (ERATO), Japan Science and Technology Agency, Aichi Medical University, Aichi 480-1195, Japan, the [¶]Laboratory for Pluripotent Cell Studies, RIKEN Center for Developmental Biology, Hyogo 650-0047, Japan, the [‖]School of Biological Science, University of Liverpool, Liverpool L69 7ZB, United Kingdom, and the **School of Biomedical Science, University of Liverpool, Liverpool L69 3GE, United Kingdom*

Basement membranes (BMs) have been implicated in cell fate determination during development. Embryoid bodies (EBs) derived from mouse embryonic stem cells deficient in the laminin γ1 chain are incapable of depositing a BM, resulting in failure of primitive ectoderm epithelialization. To elucidate the mechanisms involved in this phenomenon, we compared the gene expression profiles of EBs with or without a BM to identify the genes showing BM-dependent expression. We found that the expressions of marker genes for the epithelial-mesenchymal transition (EMT), including the transcription factor *Snai2*, were up-regulated in *LAMC1*$^{-/-}$ EBs, whereas restoration of a BM to *LAMC1*$^{-/-}$ EBs suppressed the up-regulation of these genes. Overexpression of *Snai2* induced the EMT in control EBs by molecular and morphological criteria, suggesting that suppression of the EMT regulatory genes is involved in BM-dependent epithelialization of primitive ectoderm. Despite the failure of primitive ectoderm epithelialization in BM-deficient EBs, mesodermal differentiation was not compromised, but rather accelerated. Furthermore, at later stages of control EB differentiation, the BM was disrupted at the gastrulation site where mesodermal markers were strongly expressed only in cells that had lost contact with the BM. Taken together, these results indicate that the BM prevents the EMT and precocious differentiation of primitive ectoderm toward mesoderm in EBs, implying that BMs are important for the control of mammalian gastrulation.

The differentiation and fate of many cell types are controlled by interactions with their surrounding microenvironment, of which extracellular matrix (ECM)[3] is one of the main components (1). Basement membranes (BMs) are thin sheets of ECM that directly interact with many cell types, including epithelial cells, endothelial cells, muscle cells, fat cells, and glial cells (2). Recently, targeted disruptions of BM components have revealed important roles for BMs in cell differentiation and fate determination (3). For example, disruption of the mouse laminin α5 chain, which is normally expressed in many fetal and adult tissues, leads to defects in BM integrity that result in defective morphogenesis of renal glomeruli, hair follicles, and teeth (4–7). Furthermore, deficiency of both nidogen-1 and nidogen-2 in mice also causes structural abnormalities in BMs, leading to differentiation defects in the lungs with extensive retention of mesenchyme (8). However, the mechanisms by which BMs control morphogenesis and cell fate during development still remain largely unknown.

During the early stages of mammalian development, embryonic cells must be allocated to one of the three germ layers, *i.e.* ectoderm, mesoderm, or endoderm. This process begins in the peri-implantation blastocyst when cells at the periphery of the inner cell mass (ICM) differentiate to form an extraembryonic primitive endoderm and deposit a BM that separates them from the remaining cells of the ICM, from which the germ layers are subsequently derived (9, 10). Undifferentiated ICM cells in contact with this BM become polarized and differentiate to form the primitive ectoderm epithelium. Moreover, studies using embryonic stem (ES) cell-derived embryoid bodies (EBs) have provided evidence that any unpolarized cells failing to contact the BM undergo apoptosis, leading to similar cavitation to that seen during proamniotic cavity formation (11–13). The subsequent developmental stage of gastrulation leading to mesoderm and embryonic endoderm formation involves an epithelial-mesenchymal transition (EMT), in which cells of the columnar primitive ectoderm epithelium delaminate and migrate into the space between the primitive ectoderm and extraembryonic endoderm (14). During gastrulation, the BM deposited by the primitive endoderm becomes discontinuous, probably permitting the establishment of mesodermal and embryonic endodermal layers that are spatially distinct from the remaining primitive ectoderm (14, 15; see also supplemental Fig. S1). Thus, BM

* The costs of publication of this article were defrayed in part by the payment of page charges. This article must therefore be hereby marked "*advertisement*" in accordance with 18 U.S.C. Section 1734 solely to indicate this fact.

[S] The on-line version of this article (available at http://www.jbc.org) contains supplemental Figs. S1–S4 and Tables S1 and S2.

[1] Present address: Dept. of Genetics, Research Institute of Environmental Medicine, Nagoya University, Aichi 464-8601, Japan. To whom correspondence may be addressed. Tel.: 81-52-789-3874; Fax: 81-52-789-3876; E-mail: hayashiy@riem.nagoya-u.ac.jp.

[2] To whom correspondence may be addressed. Tel.: 81-6-6879-8617; Fax: 81-6-6879-8619; E-mail: sekiguch@protein.osaka-u.ac.jp.

[3] The abbreviations used are: ECM, extracellular matrix; 4-OHT, 4-hydroxytamoxifen; BM, basement membrane; EB, embryoid body; EMT, epithelial-mesenchymal transition; ES, embryonic stem; ICM, inner cell mass; PBS, phosphate-buffered saline; SMA, smooth muscle actin; RT, reverse transcription; TUNEL, terminal deoxynucleotidyl transferase-mediated dUTP nick end labeling; E, embryonic day.

formation and integrity are dynamically regulated during germ-layer specification, although little is known about the functional relationships between the dynamic behavior of BMs and the cell differentiation and fate determination during germ-layer specification.

To investigate the roles of BMs during early embryonic development, ES cells and mice with a disrupted *LAMC1* gene have been established (10). In the absence of the laminin γ1 subunit encoded by this gene, a functional laminin trimer comprising α, β, and γ chains cannot be assembled, resulting in the absence of BMs during peri-implantation development and in EBs derived from *LAMC1*$^{-/-}$ ES cells (10). Mice heterozygous for the mutation show a normal phenotype and are fertile, whereas homozygous mutant embryos die at E5.5, mostly due to disorganization of the parietal yolk sac (10). Because *LAMC1*$^{-/-}$ mutant embryos die at E5.5, it has been difficult to analyze the roles of BMs in cell differentiation and fate determination during germ-layer specification *in vivo*. However, studies on EBs derived from *LAMC1*$^{-/-}$ ES cells have revealed that differentiation of a columnar primitive ectoderm epithelium and cavitation are dependent on BM formation (12, 13). Because the differentiation of a primitive ectoderm is dependent on BM formation, differentiating *LAMC1*$^{-/-}$ EBs provides a suitable experimental model for analyzing the consequences of the absence of a BM and addressing the mechanisms of BM-dependent cell fate determination during germ-layer specification.

In the present study, we analyzed the gene expression profiles of EBs developing with and without a BM and extended the previous observations to later stages of EB development, including the generation of mesodermal cells. Our results show that absence or disruption of the BM during EB differentiation promotes the differentiation of mesodermal cells and that BM disruption is associated with a localized EMT. These observations suggest that cell-BM interactions are responsible for normal regulation of the EMT and therefore play fundamental roles in mammalian gastrulation.

EXPERIMENTAL PROCEDURES

ES Cell and EB Cultures—The production and cultivation of R1 mouse *LAMC1*$^{+/-}$ and *LAMC1*$^{-/-}$ ES cells (10) as well as EB formation by the ES cells (12) were described in detail in the cited reports. Briefly, for EB formation, ES cells were dissociated with 0.25% trypsin/0.5 mM EDTA (Invitrogen) and plated on gelatin-coated dishes for 1–1.5 h to eliminate feeder cells that preferentially attached to the substrate. Floating ES cells were collected, plated at 2×10^5 cells/ml in 0.05% Pluronic (Sigma)-coated 60-mm bacterial Petri dishes without leukemia inhibitory factor and fed with fresh culture medium every 2 days. On day 8 of the culture period, 83.2 ± 7.3% of the *LAMC1*$^{+/-}$ EBs formed a columnar primitive ectoderm, compared with only 10.7 ± 1.1% of the *LAMC1*$^{-/-}$ EBs. For BM-rescue experiments, *LAMC1*$^{-/-}$ EBs were plated in medium containing 35 μg/ml of purified mouse laminin-111 (Sigma). The efficiency of primitive ectoderm formation in BM-rescue experiments was low (only 20–30% of the total EBs), compared with control *LAMC1*$^{+/-}$ EBs. Because most of the EBs without a cavity failed to organize BMs, we removed EBs without a cavity under a microscope to roughly normalize the efficiencies of primitive ectoderm formation between control and BM-rescued EBs. On day 8 of the culture period, 59.8 ± 10.8% of the BM-rescued *LAMC1*$^{-/-}$ EBs formed a columnar primitive ectoderm.

Antibodies and Immunofluorescence—The antibodies used in this study were: rabbit anti-mouse type IV collagen (LSL, Tokyo, Japan); rat anti-mouse laminin γ1 chain (MAB1914, Chemicon, Temecula, CA); mouse anti-α-smooth muscle actin (SMA) (ASM-1, Progen, Heidelberg, Germany); goat anti-human fibronectin (ICN, Costa Mesa, CA); goat anti-human brachyury (sc-17743, Santa Cruz Biotechnology, Santa Cruz, CA); rabbit anti-human cleaved caspase-3 (5A1, Cell Signaling, Danvers, MA); and mouse anti-FLAG M2 (Sigma).

For immunofluorescence staining, EBs were fixed with 4% paraformaldehyde in phosphate-buffered saline (PBS) for 30 min, washed in PBS, soaked in 15% sucrose in PBS for 1 h, embedded in Tissue-Tek OCT compound, and frozen in an aluminum rack floating on liquid nitrogen. Frozen sections (8 μm thick) of the EBs were blocked with 10% fetal calf serum and 1% bovine serum albumin in PBS for 30 min, and then incubated with a primary antibody diluted in the blocking solution for 1.5 h at room temperature. Next, the sections were washed with PBS and incubated with an appropriate secondary antibody conjugated with Alexa Fluor 488 (Molecular Probes, Eugene, OR) or Alexa Fluor 546 (Molecular Probes) diluted in the blocking solution, together with Hoechst 33342 (Molecular Probes) to stain the nuclei or rhodamine-phalloidin (Molecular Probes) to stain F-actin, for 1 h at room temperature. Finally, the sections were washed in PBS, mounted in a fluorescence mounting medium (Dako, Glostrup, Denmark), and photographed using an LSM5 PASCAL confocal laser scanning microscope (Zeiss, Oberkochen, Germany).

To quantify the frequency of BM formation, primitive ectoderm formation and apicolateral F-actin accumulation in EB development, we stained more than 33 frozen sections of EBs with an anti-mouse laminin γ1 chain antibody (MAB1914) and rhodamine-phalloidin in each of three separate experiments (>100 EBs in total) and counted the EBs that fulfilled the following criteria: 1) the anti-laminin γ1 chain antibody produced continuous thin sheet-like staining (BM formation); 2) primitive ectoderm cells showed a cuboidal epithelial morphology upon staining with rhodamine-phalloidin (primitive ectoderm formation); and 3) rhodamine-phalloidin staining showed F-actin accumulation at the apicolateral domain in primitive ectoderm cells (apicolateral F-actin accumulation). Representative positive staining patterns for these criteria are shown in Fig. 1 (*A–L*).

Gene Expression Profiling—Total RNA was prepared from triplicate samples of *LAMC1*$^{+/-}$, *LAMC1*$^{-/-}$, and BM-rescued *LAMC1*$^{-/-}$ EBs at day 8 using an RNeasy Mini Kit (Qiagen) combined with RNase-free DNase (Qiagen). Fluorescently labeled cRNAs were synthesized from the total RNAs and hybridized with Mouse Development Oligo Microarrays (Agilent, Palo Alto, CA) as previously described (16). Cy3-labeled cRNAs from *LAMC1*$^{-/-}$ EBs were hybridized together with Cy5-labeled cRNAs from *LAMC1*$^{+/-}$ EBs or Cy5-labeled cRNAs from BM-rescued *LAMC1*$^{-/-}$ EBs. All these hybridiza-

tions were carried out using three independent cRNA samples in triplicate experiments. The hybridized arrays were scanned using a Gene Pix 4000B (Axon Instruments, Foster City, CA). Three unscaled independent raw data sets from the triplicate experiments were loaded onto Genespring 6.0 (Silicon Genetics, Redwood City, CA) and normalized using the per-spot and per-chip intensity-dependent LOWESS method (17). The triplicate data sets that passed quality control were averaged, and then filtered using the Genespring Advanced Filtering Tool. Spots that ranked in the top 500 up-regulated or down-regulated genes were identified in *LAMC1*$^{-/-}$ EBs in comparison with *LAMC1*$^{+/-}$ EBs based on the -fold change values. The same analysis was performed against BM-rescued *LAMC1*$^{-/-}$ EBs. The genes ranking in the top 500 up-regulated gene groups in *LAMC1*$^{-/-}$ EBs in comparison with both *LAMC1*$^{+/-}$ EBs and BM-rescued *LAMC1*$^{-/-}$ EBs were identified using a Venn diagram analysis. The same analysis was performed for the down-regulated gene groups.

Quantitative RT-PCR—Total RNA was extracted and reverse-transcribed with a SuperScript III First-Strand Synthesis System for RT-PCR (Invitrogen) using random hexamer primers. The resulting cDNAs were used for PCR with SYBR Green PCR Master Mix (Applied Biosystems). PCR amplifications and data collection were performed using an ABI7000 real-time PCR system (Applied Biosystems). All quantifications were normalized by the endogenous expression levels of *Gapdh*. The relative expression levels from triplicate experiments were averaged and expressed as the mean ± S.D. The sequences of the primers are available on request.

Plasmid Construction—To construct Cre recombinase-dependent expression systems for *Snai2* and *Twist2*, we employed the pCAG-CY vector, which contains a CAG expression unit (18), a floxed puromycin-ECFP fusion protein cDNA with a stop cassette and a NotI cloning site fused to an IRES-EYFP cDNA. The entire coding regions of *Snai2* and *Twist2* were amplified by RT-PCR from total RNA extracted from *LAMC1*$^{-/-}$ EBs cultured for 10 days and subcloned into the NotI site of pCAG-CY. Both these transgenes were subsequently activated with EYFP after excision of the ECFP cassette by Cre recombinase. A FLAG tag sequence was fused in-frame to the 3′-ends of the *Snai2* and *Twist2* cDNAs. For 4-hydroxytamoxifen (4-OHT)-induced translocation of Cre recombinase to nuclei, a cDNA encoding Cre recombinase flanked by a mutated hormone-binding domain of estrogen receptor, designated MerCreMer, was excised from pCAGGS-MerCreMer (a kind gift from Dr. Mitsuhiro Endoh, Research Center for Allergy and Immunology, RIKEN, Japan) using EcoRI and subcloned into the XhoI site of pPyCAGIRESzeocinpA (19), yielding pPyCAGIRESzeocinpA-MerCreMer.

4-OHT-inducible Expression of Snai2 or Twist2 in ES Cells—The pCAG-CY vectors carrying *Snai2* and *Twist2* (pCAG-CY-*Snai2* and pCAG-CY-*Twist2*, respectively) were introduced into *LAMC1*$^{+/-}$ ES cells by electroporation using a Mouse ES Cell Nucleofector Kit (Amaxa, Cologne, Germany). The electroporated ES cells were selected with 4 μg/ml puromycin, and resistant colonies were isolated and analyzed for their expression levels of ECFP under a fluorescence microscope. ES cell clones strongly expressing ECFP were further transfected with pPyCAGIRESzeocinpA-MerCreMer, followed by selection with 40 μg/ml Zeocin. Resistant colonies were isolated and grown in the presence or absence of 0.1 μM 4-OHT (Sigma) for 24 h and stained with an anti-FLAG antibody. ES cell clones expressing FLAG and EYFP in the presence of 4-OHT were selected.

RESULTS

Gene Expression Profiling of EBs Derived from LAMC1$^{-/-}$ *and LAMC1*$^{+/-}$ *ES Cells*—EBs were produced in suspension cultures of ES cells in Petri dishes without leukemia inhibitory factor. Both *LAMC1*$^{+/-}$ and *LAMC1*$^{-/-}$ ES cells aggregated to form spheroids, *i.e.* EBs, after 1–2 days in suspension culture (Fig. 1, *A* and *A*′). At this stage, no BMs were detected in either type of EB (Fig. 1, *E* and *E*′). Shortly after the cell aggregation, the outer cells of the EBs differentiated into primitive endoderm cells, as noted by the appearance of epithelial cells at the periphery of the EBs (Fig. 1, *B* and *B*′) and expression of type IV collagen (Fig. 1, *F* and *F*′). Although *LAMC1*$^{+/-}$ EBs organized a BM containing laminin and type IV collagen between the inner cells and the peripheral primitive endoderm layer (Fig. 1*F*), no BM was detected in *LAMC1*$^{-/-}$ EBs (Fig. 1*F*′). Consistent with a previous report (12), the inner cells in contact with the BM in *LAMC1*$^{+/-}$ EBs became polarized and differentiated to form a columnar primitive ectoderm epithelium, while the unpolarized inner cells failing to contact the BM underwent apoptosis, thereby producing a central cavity by days 6–8 (Fig. 1, *C*, *D*, *G*, and *H*). Concomitant with the primitive ectoderm differentiation and cavitation, F-actin accumulated at the apicolateral domain of the primitive ectoderm cells and was lost from regions of cell-BM contact in *LAMC1*$^{+/-}$ EBs (Fig. 1, *K* and *L*). These changes in the F-actin distribution are indicative of epithelial cell polarization. On the other hand, *LAMC1*$^{-/-}$ EBs failed to form a columnar primitive ectoderm or central cavity (Fig. 1*D*′). Furthermore, F-actin did not accumulate at the apicolateral domain, but was rather distributed uniformly around the unpolarized cells in *LAMC1*$^{-/-}$ EBs (Fig. 1, *K*′ and *L*′).

To study the mechanisms underlying the BM-dependent primitive ectoderm differentiation, we compared the gene expression profiles of EBs at day 8 by cDNA microarray analysis. Because the differences in their gene expression profiles could partly result from clonal variations between the *LAMC1*$^{-/-}$ and *LAMC1*$^{+/-}$ ES cells, rather than the absence of a BM, we rescued the BM formation in *LAMC1*$^{-/-}$ EBs by supplementing the EB cultures with exogenous laminin-111 and compared the gene expression profile of BM-rescued *LAMC1*$^{-/-}$ EBs with that of nonrescued *LAMC1*$^{-/-}$ EBs. As shown previously (12), *LAMC1*$^{-/-}$ EBs cultured with laminin-111 organized a BM, and produced a columnar primitive ectoderm and central cavity (Fig. 1, *M*–*O*). Furthermore, F-actin accumulated at the apicolateral domain of the primitive ectoderm in BM-rescued *LAMC1*$^{-/-}$ EBs (Fig. 1*P*), demonstrating that the actin cytoskeleton dynamics in primitive ectoderm formation are dominated by the BM. Thus, comparison of the gene expression profile of *LAMC1*$^{-/-}$ EBs with those of *LAMC1*$^{+/-}$ EBs and BM-rescued *LAMC1*$^{-/-}$ EBs allowed us to focus on the BM-responsive genes and eliminate false-positive genes reflect-

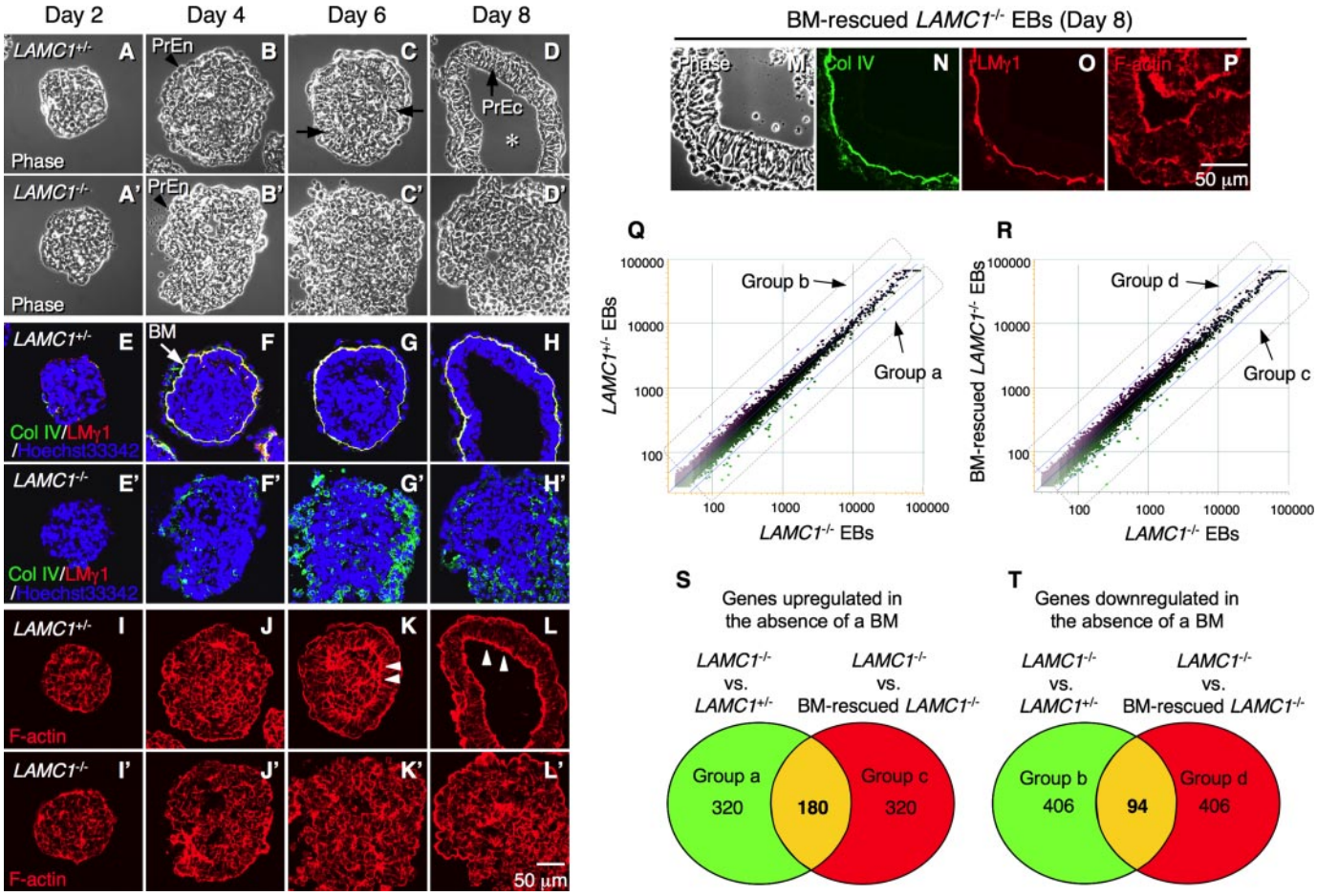

FIGURE 1. **Microarray-based screening for BM-responsive genes.** *A–L* and *A′–L′*, development of EBs derived from *LAMC1*$^{+/-}$ and *LAMC1*$^{-/-}$ ES cells. *LAMC1*$^{+/-}$ and *LAMC1*$^{-/-}$ ES cells were cultured as EBs for 8 days. *A–D* and *A′–D′*, phase-contrast images of *LAMC1*$^{+/-}$ and *LAMC1*$^{-/-}$ EBs. *E–H* and *E′–H′*, Fluorescence images of type IV collagen (*green*), laminin γ1 chain (*red*) and nuclei (*blue*) in *LAMC1*$^{+/-}$ and *LAMC1*$^{-/-}$ EBs. *I–L* and *I′–L′*, fluorescence images of F-actin (*red*) in *LAMC1*$^{+/-}$ and *LAMC1*$^{-/-}$ EBs. On day 4, cells on the surface of both *LAMC1*$^{+/-}$ and *LAMC1*$^{-/-}$ EBs become differentiated into a primitive endoderm (PrEn; *black arrowheads* in *B* and *B′*), although a BM is only present in *LAMC1*$^{+/-}$ EBs (*F* and *F′*). On day 6, inner cells adhering to the BM in *LAMC1*$^{+/-}$ EBs begin to polarize and form a columnar primitive ectoderm (*black arrows* in *C*) and accumulate F-actin at their apicolateral domain (*white arrowheads* in *K*), whereas inner cells in *LAMC1*$^{-/-}$ EBs show unpolarized morphologies (*C′*) and uniform distribution of F-actin (*K′*). On day 8, the unpolarized primitive ectoderm in the center of *LAMC1*$^{+/-}$ EBs undergoes apoptosis, yielding a central cavity (*asterisk* in *D*) and single-layer primitive ectoderm sheet (*PrEc* in *D*). F-actin accumulates at the apicolateral surface of the primitive ectoderm in *LAMC1*$^{+/-}$ EBs (*white arrowheads* in *L*). However, no central cavity or single-layer primitive ectoderm sheet is formed in *LAMC1*$^{-/-}$ EBs (*D′*). The distribution of F-actin in the prospective primitive ectoderm does not change during *LAMC1*$^{-/-}$ EB differentiation (*I′–L′*). *M–P*, rescue of *LAMC1*$^{-/-}$ EBs by addition of exogenous laminin. *LAMC1*$^{-/-}$ ES cells were cultured as EBs for 8 days in the presence of 35 μg/ml mouse laminin-111 to rescue the BM. Phase-contrast image of BM-rescued *LAMC1*$^{-/-}$ EBs (*M*). The BM-rescued *LAMC1*$^{-/-}$ EBs were stained with antibodies against type IV collagen (*N*) and laminin γ1 chain (*O*), and with rhodamine-phalloidin for F-actin (*P*). *Q* and *R*, scatter plots of the cDNA microarray spot statistics. The fluorescence intensity of the labeled cRNA in each spot was plotted on a logarithmic scale (*Q*: *LAMC1*$^{-/-}$ EBs *versus* *LAMC1*$^{+/-}$ EBs; *R*: *LAMC1*$^{-/-}$ EBs *versus* BM-rescued *LAMC1*$^{-/-}$ EBs). Each data point represents the mean of three independent experiments. Based on the expression levels of each gene in the *LAMC1*$^{-/-}$, *LAMC1*$^{+/-}$, and BM-rescued *LAMC1*$^{-/-}$ EBs, the top 500 genes either up-regulated (*group a*) or down-regulated (*group b*) in *LAMC1*$^{-/-}$ EBs compared with *LAMC1*$^{+/-}$ EBs were selected. Similarly, the top 500 genes either up-regulated (*group c*) or down-regulated (*group d*) in *LAMC1*$^{-/-}$ EBs compared with BM-rescued *LAMC1*$^{-/-}$ EBs were selected. *S* and *T*, Venn diagram analyses of the genes up-regulated (*S*) or down-regulated (*T*) in the absence of a BM. To identify genes responsive to the absence of a BM, the genes included in both *groups a* and *c* (*S*) or *groups b* and *d* (*T*) were extracted by the Venn diagram analyses.

ing clonal variation between *LAMC1*$^{-/-}$ and *LAMC1*$^{+/-}$ ES cells.

Genes whose expression profiles changed in the absence of a BM were delineated as follows. We selected the top 500 genes that were either up-regulated (group a) or down-regulated (group b) in *LAMC1*$^{-/-}$ EBs compared with *LAMC1*$^{+/-}$ EBs (Fig. 1*Q*). Similarly, we selected the top 500 genes whose expression levels were higher (group c) or lower (group d) in *LAMC1*$^{-/-}$ EBs than in BM-rescued *LAMC1*$^{-/-}$ EBs (Fig. 1*R*). A Venn diagram was used to extract the genes included in groups a and c (Fig. 1*S*) or groups b and d (Fig. 1*T*). As a result, 180 genes were identified as being up-regulated in the absence of a BM (supplemental Table S1), while 94 genes were down-regulated in the absence of a BM (supplemental Table S2).

Up-regulation of EMT-related Genes in LAMC1$^{-/-}$ *EBs*—Near the top of the list of genes up-regulated in the absence of a BM, we found a group of genes related to the EMT, including EMT inducers and markers (Table 1). For example, IGF-2 has been reported to induce the EMT in ES cells (20), whereas cell adhesion-related genes, such as *Vim* (vimentin), *Acta2* (α-SMA), and *Fn1* (fibronectin), are well known as mesenchymal marker genes induced during the EMT (21). Quantitative RT-PCR analyses confirmed that *Igf2* (IGF-2), *Tgfb2* (TGFβ-2), *Fn1*, *Vim*, and *Acta2* were more strongly expressed in

TABLE 1
EMT-related genes up-regulated in the absence of a BM

	Change (S.D.)[a]	
	LAMC1$^{-/-}$ *vs.* BM-rescued *LAMC1*$^{-/-}$	*LAMC1*$^{-/-}$ *vs.* *LAMC1*$^{+/-}$
	-fold	
Signaling molecules		
Igf2 (insulin-like growth factor 2)	2.8 (0.3)	3.8 (0.8)
Tgfb2 (transforming growth factor, β2)	1.7 (0.4)	1.3 (0.2)
Wnt5a (wingless-related MMTV integration site 5A)	1.6 (0.3)	1.3 (0.1)
Cell adhesion-related		
Myl4 (myosin, light polypeptide 4, alkali, atrial, embryonic)	1.9 (0.4)	2.9 (0.5)
Fn1 (fibronectin 1)	1.8 (0.2)	1.5 (0.2)
Vim (vimentin)	1.8 (0.1)	2.3 (0.5)
Acta2 (actin, α2, smooth muscle, aorta)	1.8 (0.3)	2.1 (0.6)
Cdh11 (cadherin 11)	1.6 (0.1)	1.6 (0.1)
Transcription factors		
Ets2 (E26 avian leukemia oncogene 2, 3′ domain)	1.7 (0.3)	1.5 (0.2)
Etv5 (Ets variant gene *5*)	1.6 (0.4)	1.6 (0.3)

[a] Values are the means ± S.D.s of three independent experiments.

LAMC1$^{-/-}$ EBs than in *LAMC1*$^{+/-}$ EBs at day 8, while the up-regulation of these genes was suppressed when the BM was rescued by exogenously added laminin-111 (Fig. 2, *A–E*). It should also be noted that up-regulation of these EMT-related genes was not evident at day 4, when a BM was detectable in *LAMC1*$^{+/-}$ EBs, but became pronounced at day 6 in *LAMC1*$^{-/-}$ EBs. This delayed up-regulation of the EMT-related genes, relative to the onset of BM deposition by the primitive endoderm, raised the possibility that the up-regulation of EMT-related genes in *LAMC1*$^{-/-}$ EBs was triggered by the absence of a BM.

To verify the up-regulation of mesenchymal markers in *LAMC1*$^{-/-}$ EBs at the protein level, we stained *LAMC1*$^{+/-}$, *LAMC1*$^{-/-}$, and BM-rescued *LAMC1*$^{-/-}$ EBs with antibodies against α-SMA and fibronectin. α-SMA was strongly detected in the inner cells, *i.e.* the prospective primitive ectoderm, of *LAMC1*$^{-/-}$ EBs (Fig. 2*G*), but less so in *LAMC1*$^{+/-}$ and BM-rescued *LAMC1*$^{-/-}$ EBs (Fig. 2, *F* and *H*), clearly reflecting the remarkable changes in its mRNA level detected by quantitative RT-PCR. Fibronectin was also detected in *LAMC1*$^{-/-}$ EBs, with prominent deposition in the ECM between prospective primitive ectoderm cells (Fig. 2*J*), whereas the staining for fibronectin was less prominent and restricted to the BM in *LAMC1*$^{+/-}$ and BM-rescued *LAMC1*$^{-/-}$ EBs (Figs. 2, *I* and *K*). These results are consistent with those obtained in the cDNA microarray and quantitative RT-PCR analyses and indicate that the absence of a BM during EB differentiation induces up-regulation of mesenchymal markers in the prospective primitive ectoderm after the BM formation stage.

Up-regulation of Snai2 and Twist2 in LAMC1$^{-/-}$ *EBs*—The expressions of mesenchymal genes, such as *Acta2* and *Fn1*, during the EMT are known to be regulated by the Snail and Twist families of transcription factors (22, 23). These transcription factors play central roles in the EMT as master regulators during embryonic development and cancer progression (22, 23). To examine whether the absence of a BM induces these master regulators of the EMT, we investigated the expression levels of *Snai1* (Snail1), *Snai2* (Snail2/Slug), *Snai3* (Snail3), *Twist1* and *Twist2* in *LAMC1*$^{+/-}$, *LAMC1*$^{-/-}$, and BM-rescued *LAMC1*$^{-/-}$ EBs by quantitative RT-PCR. Among the Snail family of transcription factors, the expression of *Snai2* was greater in *LAMC1*$^{-/-}$ EBs than in *LAMC1*$^{+/-}$ and BM-rescued *LAMC1*$^{-/-}$ EBs (Fig. 3*B*). *Twist2* was also significantly up-regulated in *LAMC1*$^{-/-}$ EBs (Fig. 3*E*). The differences in the expression levels of *Snai1*, *Snai3*, and *Twist1* between EBs with and without a BM were only marginal (Fig. 3, *A*, *C*, and *D*). Elevated expression of *Snai2* in *LAMC1*$^{-/-}$ EBs was also detected in microarray analyses, scoring 1.42- and 1.12-fold increases compared with BM-rescued *LAMC1*$^{-/-}$ EBs and *LAMC1*$^{+/-}$ EBs, respectively. *Twist2* was not included in the repertoire of the microarray used. These observations indicate that the absence of a BM activates upstream EMT regulators in ES cells as EB differentiation proceeds.

To explore whether the up-regulation of *Snai2* or *Twist2* was capable of inhibiting the columnar primitive ectoderm formation and inducing the mesenchymal phenotype in *LAMC1*$^{-/-}$ EBs, we overexpressed *Snai2* or *Twist2* in *LAMC1*$^{+/-}$ EBs and examined their effects on EB differentiation. To exclude the influence of overexpression of *Snai2* or *Twist2* on earlier stages of EB differentiation, we constructed a 4-OHT-inducible expression system of *Snai2* or *Twist2* utilizing MerCreMer, which efficiently induced Cre-mediated DNA recombination in ES cells in a 4-OHT-dependent manner (24). Combining the MerCreMer expression vector (pPyCAGIRESzeocinpA-MerCreMer) with the pCAG-CY vector, which is designed for Cre recombinase-dependent gene expression, we constructed 4-OHT-inducible expression systems for *Snai2* and *Twist2* in *LAMC1*$^{+/-}$ ES cells. Cells stably carrying pPyCAGIRESzeocinpA-MerCreMer together with pCAG-CY-*Snai2* or pCAG-CY-*Twist2* were allowed to form EBs and then treated with 0.1 μM 4-OHT on day 4 of the EB culture. The expression of *Snai2* or *Twist2* was strongly induced on days 6 and 8 of the EB culture (Fig. 3, *F* and *H*). In 4-OHT-treated *Snai2* EBs, primitive ectoderm epithelialization (Fig. 3, *J*, *K*, and *V*) and apicolateral F-actin accumulation (Fig. 3, *N*, *O*, and *V*) were significantly inhibited ($p < 0.001$). Furthermore, overexpression of *Snai2* induced the expression of the mesenchymal marker gene *Acta2* (Fig. 3*G*). Although overexpression of *Twist2* in *LAMC1*$^{+/-}$ EBs also suppressed primitive ectoderm epithelialization (Fig. 3, *L*, *M*, and *W*, $p < 0.05$) and apicolateral F-actin accumulation (Fig. 3, *P*, *Q*, and *W*, $p < 0.05$), its inhibitory effects on primitive ectoderm formation, as well as up-regulatory effects on *Acta2* expression (Fig. 3*I*), were less prominent than those observed in the *Snai2* transfectants. It should also be noted that a BM was formed in the 4-OHT-treated *Snai2* EBs, although its thickness was irregular (Fig. 3, *R* and *S*). Taken together, these results indicate that the absence of a BM during EB differentiation activates *Snai2* and *Twist2*, the upstream regulators of the EMT, and that overexpression of *Snai2* could in turn trigger the EMT cascade, leading to failure of primitive ectoderm epithelialization and induction of a mesenchymal phenotype in *LAMC1*$^{-/-}$ EBs.

Accelerated Mesodermal Differentiation in LAMC1$^{-/-}$ *EBs*—In the early stages of mouse embryonic development, the mesoderm is generated from the primitive ectoderm at gastrulation

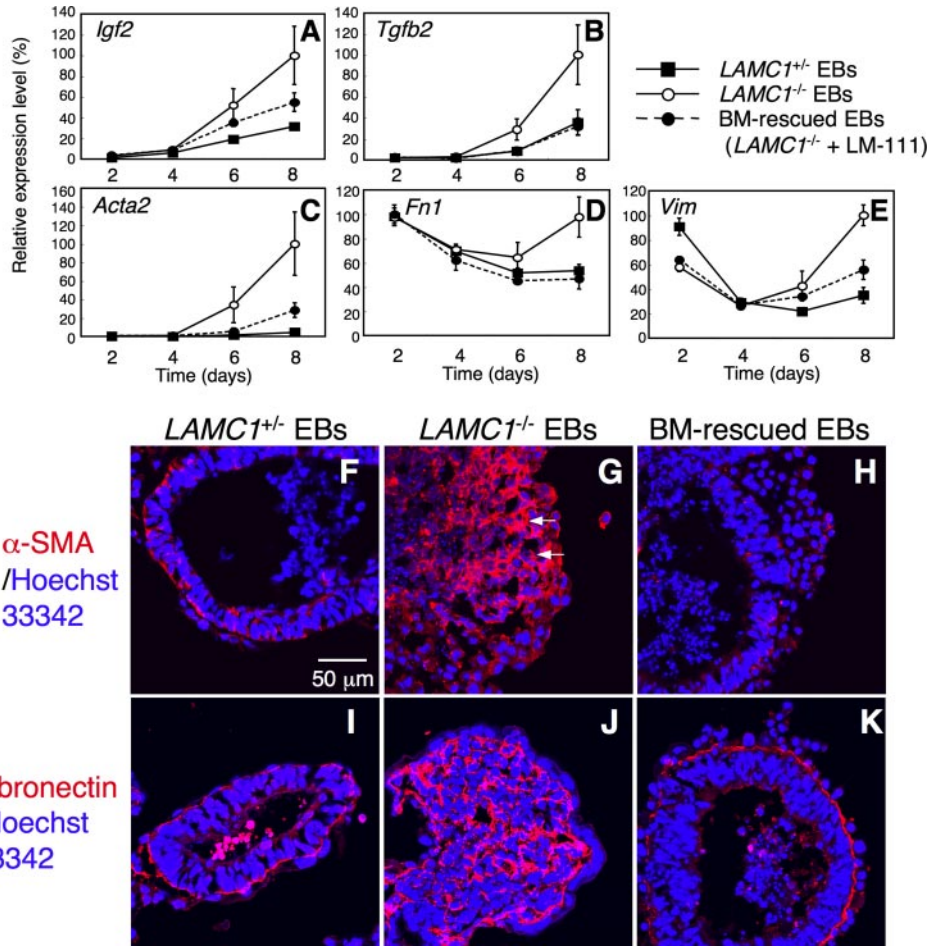

FIGURE 2. **Up-regulation of EMT-related genes in *LAMC1*$^{-/-}$ EBs.** *A–E*, time courses of the expressions of mesenchymal marker genes for the EMT. The expression levels of *Igf2* (*A*), *Tgfb2* (*B*), *Acta2* (*C*), *Fn1* (*D*), and *Vim* (*E*) transcripts were determined by quantitative RT-PCR. The mesenchymal marker genes are up-regulated in *LAMC1*$^{-/-}$ EBs. Each data point represents the mean ± S.D. of three independent dishes. *F–H*, immunohistochemical staining of *LAMC1*$^{+/-}$ (*F*), *LAMC1*$^{-/-}$ (*G*), and BM-rescued *LAMC1*$^{-/-}$ (*H*) EBs at day 8 with an antibody against α-SMA (*red*). The *arrows* in *G* indicate strong expression of α-SMA in the cytoplasm of prospective primitive ectoderm of *LAMC1*$^{-/-}$ EBs. Nuclei were stained with Hoechst 33342 (*blue*). *I–K*, immunohistochemical staining of *LAMC1*$^{+/-}$ (*I*), *LAMC1*$^{-/-}$ (*J*), and BM-rescued *LAMC1*$^{-/-}$ (*K*) EBs at day 8 with an antibody against fibronectin (*red*). In the presence of a BM (*LAMC1*$^{+/-}$ and BM-rescued *LAMC1*$^{-/-}$ EBs), staining for fibronectin is restricted to the BM zone. In the absence of a BM (*LAMC1*$^{-/-}$ EBs), however, the staining for fibronectin is prominent and detected between prospective primitive ectoderm cells.

by the EMT process (14). Given the accelerated expression of EMT-related genes in *LAMC1*$^{-/-}$ EBs, it seemed likely that mesodermal differentiation was not inhibited, but rather induced and possibly accelerated, in *LAMC1*$^{-/-}$ EBs without passing through an obligatory primitive ectodermal stage that would normally be the case in gastrulation. To explore this possibility, we examined the expression levels of the following differentiation marker genes by quantitative RT-PCR: *Fgf5* for primitive ectoderm (25); *Bmp4* for ES cells, early epiblasts, and mesoderm; and *T* (brachyury) and *Cdh11* (cadherin-11) for mesoderm. Expression of *Fgf5* was induced in both *LAMC1*$^{+/-}$ and *LAMC1*$^{-/-}$ EBs and was not affected by BM restoration (Fig. 4*A*). *Bmp4* transcripts have been shown to be highly expressed in ES cells and early epiblasts, down-regulated in columnar primitive ectoderm (26), and then up-regulated in mesoderm cells as gastrulation proceeds (27, 28). *Bmp4* expression was down-regulated in *LAMC1*$^{-/-}$ EBs at day 4, similar to the case for *LAMC1*$^{+/-}$ and BM-rescued *LAMC1*$^{-/-}$ EBs. Thereafter, it was significantly up-regulated in *LAMC1*$^{-/-}$ EBs by day 8, but remained down-regulated in *LAMC1*$^{+/-}$ and BM-rescued *LAMC1*$^{-/-}$ EBs (Fig. 4*B*). The induction of *Fgf5* expression, together with the transient down-regulation of *Bmp4*, in *LAMC1*$^{-/-}$ EBs indicates that the failure of BM formation and primitive ectoderm epithelialization does not compromise the biochemical differentiation process of ES cells into primitive ectoderm cells. Furthermore, induction of the expression of the mesodermal markers *T* and *Cdh11* was accelerated in *LAMC1*$^{-/-}$ EBs, but followed the normal time course upon BM reconstitution (Fig. 4, *C* and *D*). The accelerated expressions of the mesoderm markers *Bmp4*, *T*, and *Cdh11* at later stages of EB differentiation in *LAMC1*$^{-/-}$ EBs indicate that mesodermal differentiation is not compromised, but rather accelerated, in the absence of a BM, despite the deficiency in BM-stimulated morphological changes, *i.e.* epithelialization, of primitive ectoderm cells.

BM Disruption Is Correlated with the Induction of Mesenchymal and Mesodermal Markers during the Development of EBs—The mesenchymal and mesodermal marker genes *Acta2* and *T* were induced upon prolonged culture of *LAMC1*$^{+/-}$ EBs, *e.g.* at day 10 (Fig. 5, *A* and *B*). The induction of these marker genes in *LAMC1*$^{+/-}$ EBs is indicative of the development of mesodermal cells. To investigate the role of the BM in mesoderm differentiation in normal EBs, we stained sections of *LAMC1*$^{+/-}$ EBs at day 10 with antibodies against α-SMA (*Acta2*), brachyury (*T*), and laminin γ1 chain. We observed a cluster of nonpolar round cells between the primitive ectoderm and peripheral primitive endoderm layer in *LAMC1*$^{+/-}$ EBs at day 10 (Fig. 5, *C* and *D*). These cells, which were found to arise from delamination of primitive ectoderm (see supplemental Fig. S2), were strongly positive for α-SMA and brachyury, compared with the more polarized primitive ectodermal cells (Fig. 5, *E* and *F*). Immunostaining for the laminin γ1 chain revealed disruption of the BM near the cluster of nonpolar round cells in *LAMC1*$^{+/-}$ EBs (Fig. 5, *E* and *F*), as has been observed during gastrulation *in vivo* (14; see also supplemental Fig. S1). Staining for α-SMA and brachyury was only weakly detected in primitive ectoderm cells adhering to the BM, but prominent in cells that had detached from the BM (Fig. 5, *E* and *F*). In *LAMC1*$^{-/-}$ EBs, brachyury-expressing cells were

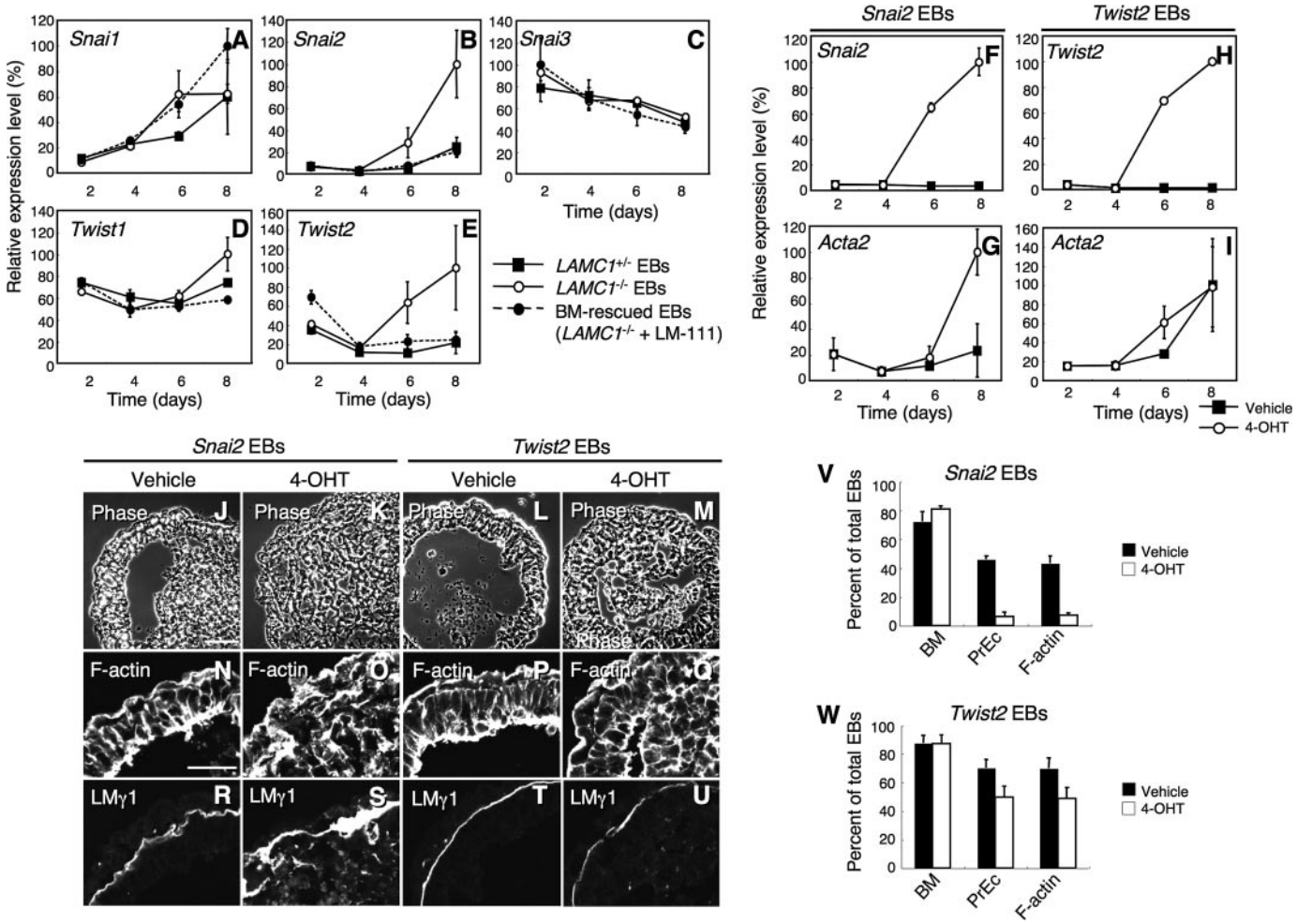

FIGURE 3. **Up-regulation of *Snai2* and *Twist2* transcription factors in *LAMC1*$^{-/-}$ EBs and effects of *Snai2* or *Twist2* overexpression on EB differentiation.** *A–E*, time courses of the expressions of the Snail and Twist families of transcription factors in *LAMC1*$^{+/-}$, *LAMC1*$^{-/-}$, and BM-rescued *LAMC1*$^{-/-}$ EBs. The expression levels of *Snai1* (*A*), *Snai2* (*B*), *Snai3* (*C*), *Twist1* (*D*), and *Twist2* (*E*) transcripts were determined by quantitative RT-PCR. *Snai2* and *Twist2* are up-regulated in *LAMC1*$^{-/-}$ EBs. Each data point represents the mean ± S.D. of three independent dishes. *F–I*, relative expression levels of *Snai2* (*F*), *Twist2* (*H*), and *Acta2* (*G* and *I*) in *LAMC1*$^{+/-}$ EBs stably carrying a 4-OHT-inducible expression system of *Snai2* (*F* and *G*: *Snai2* EBs) or *Twist2* (*H* and *I*: *Twist2* EBs). 4-OHT was applied on day 4 to induce exogenous *Snai2* or *Twist2* expression. Each data point represents the mean ± S.D. of three independent dishes. *J–U*, aberrant formation of a primitive ectoderm epithelium and cavitation in *Snai2*- or *Twist2*-overexpressing *LAMC1*$^{+/-}$ EBs. The *Snai2* or *Twist2* EBs were treated with 4-OHT on day 4. Phase-contrast (*J–M*), F-actin-stained (*N–Q*), and laminin γ1 chain-stained (*R–U*) images of the EBs at day 8 are shown. Overexpression of *Snai2* inhibits the formation of a cavity and columnar primitive ectoderm in *LAMC1*$^{+/-}$ EBs (*J*, *K*, *N*, and *O*). The effects of overexpression of *Twist2* on cavitation and columnar primitive ectoderm formation are less prominent (*L*, *M*, *P*, and *Q*). *V* and *W*, quantification of the frequencies of BM formation (*BM*), primitive ectoderm formation (*PrEc*), and apicolateral F-actin accumulation (*F-actin*) in *Snai2* and *Twist2* EBs. The data represent the mean ± S.D. of three independent experiments. *Bars* in *J* and *N* indicate 50 μm.

widely detected, but distributed randomly, rather than being clustered (Fig. 5, *G* and *H*). These results indicate that BM disruption and detachment of primitive ectodermal cells from the BM are closely associated with the induction of mesenchymal and mesodermal markers during the development of EBs. Furthermore, the random distribution of brachyury-expressing cells in *LAMC1*$^{-/-}$ EBs *versus* their restricted distribution in *LAMC1*$^{+/-}$ EBs at the site of BM disruption suggests roles for the BM in the regionalization of cell fate determination and tissue patterning in EB development.

DISCUSSION

In the present study, we have shown that the expressions of EMT-related and mesodermal marker genes are accelerated in *LAMC1*$^{-/-}$ EBs that lack a BM and fail to form a columnar primitive ectoderm. Rescue of the BM deposition in *LAMC1*$^{-/-}$ EBs by addition of exogenous laminin suppressed the expressions of these genes, concomitant with rescue of the primitive ectoderm epithelialization. At later stages of normal EB differentiation, the BM was disrupted at the site of gastrulation, as has been observed *in vivo* (14; also supplemental Fig. S1), and both mesenchymal and mesodermal markers were strongly expressed only in cells losing contact with the BM, and not in cells adhering to the BM. Based on these observations, we propose that deposition of a BM beneath a primitive endoderm not only promotes the epithelialization of prospective primitive ectoderm cells in contact with the BM (12), but also represses the expression of genes associated with mesodermal differentiation, while BM deficiency results in failure of primitive ectoderm epithelialization and permits and/or accelerates mesodermal differentiation (Fig. 6). In normal EBs, the BM subsequently undergoes regional degradation at the time of

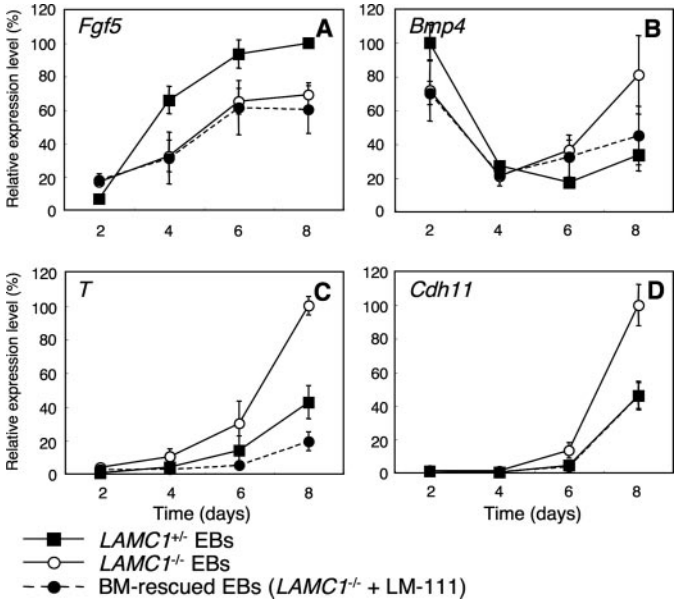

FIGURE 4. **Expression of differentiation marker genes in EBs.** *A–D*, the relative expression levels of the following differentiation marker genes in *LAMC1*$^{+/-}$, *LAMC1*$^{-/-}$, and BM-rescued *LAMC1*$^{-/-}$ EBs were determined by quantitative RT-PCR: *Fgf5*, a primitive ectoderm marker (*A*); *Bmp4*, an early primitive ectoderm and mesoderm marker (*B*); and *T* (brachyury) and *Cdh11* (cadherin-11), mesoderm markers (*C* and *D*, respectively). The expressions of the mesoderm markers (*B–D*) are accelerated in *LAMC1*$^{-/-}$ EBs. Each data point represents the mean ± S.D. of three independent dishes.

gastrulation, thereby promoting mesodermal differentiation from columnar primitive ectoderm cells via the EMT (Fig. 6).

Roles of the BM in ES Cell Differentiation—During EB differentiation, no apparent mesenchymal tissues are detectable until the mesoderm is generated by delamination of the primitive ectoderm epithelium. It has long been assumed that differentiation of epiblasts into the primitive ectoderm epithelium is an obligatory step that precedes mesodermal cell differentiation. Although *LAMC1*$^{-/-}$ EBs cannot give rise to cells that exhibit the typical epithelial morphology of primitive ectoderm, the observed expression patterns of primitive ectoderm and mesoderm marker genes in *LAMC1*$^{-/-}$ EBs indicate that biochemical differentiation of ES/ICM cells to primitive ectoderm proceeds in the absence of a BM and that primitive ectodermal cells failing to undergo epithelialization can differentiate into mesodermal cells in *LAMC1*$^{-/-}$ EBs. Thus, BM-stimulated epithelialization of primitive ectoderm is not a prerequisite for mesoderm differentiation of ES/ICM cells.

Our results also show that cells adhering to the BM during EB differentiation are resistant to mesodermal differentiation and retain the characteristics of primitive ectoderm epithelial cells, suggesting that the BM is capable of restricting the progression of primitive ectodermal cells to gastrulation. Consistent with the inhibitory effects of the BM on the progression of cell differentiation, mouse and human ES cells adhering to Matrigel™ or laminin stably retain their undifferentiated state, whereas those adhering to other substrates, such as fibronectin, do not (29, 30). Furthermore, cell-BM interactions have been shown to maintain the differentiation status of BM-adherent cells in other tissues. During myotome formation, dermomyotome cells maintain their undifferentiated state by interacting with a laminin-rich BM-like matrix through integrin $\alpha6\beta1$, prior to degradation of the BM-like matrix and their entry into the myotome (31). Conditional knock-out of the integrin $\beta1$ subunit in the central nervous system results in impaired BM formation by cerebellar granule cell precursors, reduced cell proliferation, and precocious differentiation of granule cell precursors (32). Our present results strongly suggest that the primitive ectoderm is similarly maintained through adherence to the BM. This view is in agreement with a previous observation that the mesoderm only differentiates from primitive ectoderm positioned along the primitive streak, an area of localized BM breakdown (15).

The interactions of ES cells with BMs are primarily mediated by laminin receptors, including integrin $\alpha6\beta1$ and α-dystroglycan, on the cell surface (13). Although the mechanisms governing the BM-dependent suppression of mesodermal differentiation of the primitive ectoderm remain to be elucidated, these receptors are potentially involved in the suppression of mesodermal differentiation. However, mice deficient in the integrin $\alpha6$ subunit or both the integrin $\alpha6$ and $\alpha3$ subunits were found to develop beyond the gastrulation stage (33, 34), making it unlikely that these laminin-binding integrins are prerequisites for the suppression of mesodermal differentiation. Recently, Scheele *et al.* (35) reported that EBs lacking the LG4–5 modules of the laminin $\alpha1$ chain exhibit defects in primitive ectoderm epithelialization and cavity formation, namely the same phenotypes observed in *LAMC1*$^{-/-}$ EBs, although their BM formation is not impaired. The LG4–5 modules have been shown to interact with a panel of cell surface molecules, including α-dystroglycan (36), syndecans (37), and sulfated glycolipids (38). EBs deficient in dystroglycan are capable of producing a columnar primitive ectoderm (13), arguing against a critical role for α-dystroglycan in the BM-dependent epithelialization of the primitive ectoderm. Other laminin receptors binding to the LG4–5 modules may well be involved in the process and concomitant suppression of the subsequent mesodermal differentiation. Alternatively, signaling events involved in these processes may be elicited by cooperative interactions of α-dystroglycan and other receptors, *e.g.* integrin $\alpha6\beta1$, with laminin, as recently reported for the polarization of mammary epithelial cells and β-casein production in these cells (39). Such cooperativity may lead to the absence of clear phenotypes in mice deficient in the individual receptors involved. In addition, we cannot exclude the possibility that the BM suppresses mesodermal differentiation by restricting certain signaling events elicited by soluble growth factors, morphogens and/or other ECM proteins, whose spatial distributions are restricted by binding to the BM. For example, fibronectin was mostly associated with the BM in *LAMC1*$^{+/-}$ and BM-rescued *LAMC1*$^{-/-}$ EBs, whereas it was organized into a fibrillar matrix surrounding prospective primitive ectoderm cells in *LAMC1*$^{-/-}$ EBs. Because fibronectin has been implicated in the progression of mesodermal differentiation (40, 41), the spatial restriction of fibronectin to the BM may contribute to the suppression of mesodermal differentiation of primitive ectoderm cells.

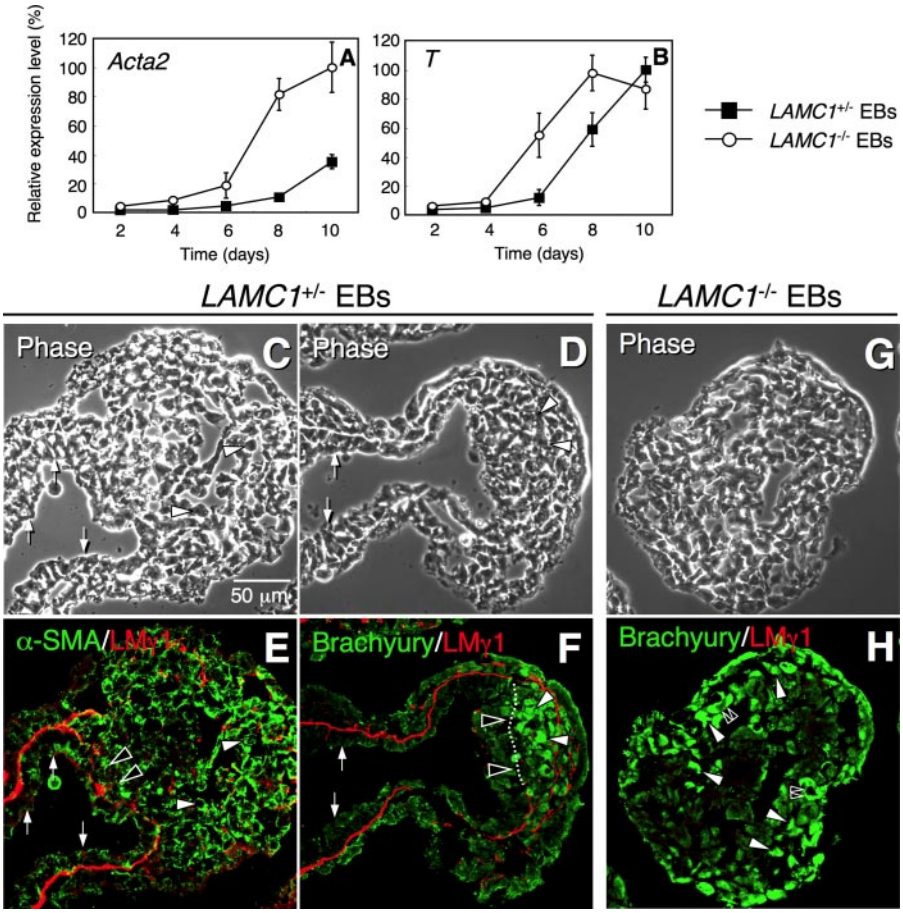

FIGURE 5. **BM disruption is correlated with the induction of mesenchymal and mesodermal markers during EB development.** *A* and *B*, time courses of the expressions of *Acta2* (α-SMA) (*A*) and *T* (brachyury) (*B*) in *LAMC1*$^{+/-}$ and *LAMC1*$^{-/-}$ EBs determined by quantitative RT-PCR. *Acta2* and *T* expressions are induced at earlier time points in *LAMC1*$^{-/-}$ EBs than in *LAMC1*$^{+/-}$ EBs. Each data point represents the mean ± S.D. of three independent dishes. *C* and *D*, phase-contrast images of *LAMC1*$^{+/-}$ EBs cultured for 10 days reveal the presence of two distinct types of primitive ectoderm cells: nonpolar round cells (*white arrowheads*) and cells retaining epithelial polarity (*white arrows*). *E* and *F*, the EBs in *C* and *D* were stained with antibodies against α-SMA (*green* in *E*), brachyury (*green* in *F*), and laminin γ1 chain (*red* in *E* and *F*). Primitive ectoderm cells that have detached from the BM and invaginated from the primitive ectoderm sheet (*white arrowheads*), but not those adhering to the BM (*white arrows*), significantly express α-SMA and brachyury. α-SMA is detected in the perinuclear/cytoplasmic region, as shown in Fig. 2*G*. Brachyury is localized in the nuclei (*white arrowheads*; see also supplemental Fig. S3), confirming the specificity of the antibody used. The *open arrowheads* in *E* and *F* point to sites of focal BM disruption. The *white dotted line* in *F* indicates the region where the BM is locally disrupted. *G*, a phase-contrast image of *LAMC1*$^{-/-}$ EBs cultured for 10 days shows nonpolar round inner cells. *H*, the EB in *G* was stained with antibodies against brachyury (*green*) and laminin γ1 chain (*red*). The brachyury-expressing cells are randomly distributed in *LAMC1*$^{-/-}$ EBs without regionalization, as observed in *LAMC1*$^{+/-}$ EBs. The brachyury-positive nuclei are often juxtaposed with each other, leaving a space that appears to be an spared nuclear area (*open double arrowheads* in *H*).

It has been shown that E5.5 *LAMC1*$^{-/-}$ embryos exhibit an increased number of TUNEL-positive cells, indicative of the increase of apoptotic cells (10). This observation raises the possibility that the mesodermal cells in *LAMC1*$^{-/-}$ EBs are terminally differentiated cells that undergo apoptosis. However, only a few randomly scattered cells were positive for TUNEL or cleaved caspase-3 at the later developmental stages of *LAMC1*$^{-/-}$ EBs (12; see also supplemental Fig. S4) and the cells positive for brachyury were not co-stained with the antibody against cleaved caspase-3 (supplemental Fig. S4), indicating that accelerated mesodermal differentiation in *LAMC1*$^{-/-}$ EBs does not occur as a consequence of apoptosis-mediated terminal cell differentiation, but rather reflects the acceleration of normal differentiation process of primitive ectoderm cells toward mesodermal cells. Although the causes of the apoptosis and involution in *LAMC1*$^{-/-}$ embryos remain unclear, our studies in EBs suggest that these processes in *LAMC1*$^{-/-}$ embryos are induced as secondary responses of the defects of *LAMC1* genes such as the absence of parietal yolk sac (10, 12). If *LAMC1*$^{-/-}$ embryos could evade these processes at early embryogenesis, they might give rise to a teratoma-like structure that is dominated by mesoderm-derived tissues at the later stages of embryogenesis.

Involvement of Cell-BM Interactions in the EMT—The current concept of the EMT postulates a mechanism in which epithelial cells become activated by exogenous stimuli, followed by loss of contact with their neighboring cells and the underlying BM (21, 42). Upon initiation of the EMT, cells move through the BM and acquire a mesenchymal phenotype (21, 42). During most of the EMT process described to date, BM disruption at the site of epithelial cell invasion has been observed (15, 21, 42, 43). However, little is known about the physiological significance of BM disruption in the EMT, because it has been difficult to manipulate the BMs in EMT models or construct intact BMs in conventional two-dimensional culture systems *in vitro*. Thus, BM disruption during the EMT has only been considered as a process that opens a route for epithelial cell invasion, and the relevance of BM disruption for the EMT has been largely neglected. The present study indicates that the absence of a BM promotes an EMT cascade in prospective primitive ectoderm cells during EB differentiation, raising the possibility that loss of contact of the epithelial cells with the BM is one of the stimulators of the EMT. This notion is consistent with a previous report by Zeisberg *et al.* (44), in which destabilization of the type IV collagen meshwork following addition of the α1NC1 domain of type IV collagen induced the EMT in mouse renal cell cultures.

During the EMT, there is a dramatic reorganization of the actin cytoskeleton, an event that is known to be an early and necessary feature of the EMT (45, 46). The EMT only proceeds if the actin cytoskeleton is excluded from cell-cell adhesion sites and recruited to cell-ECM interaction sites (47). In the present study, we have shown that these actin

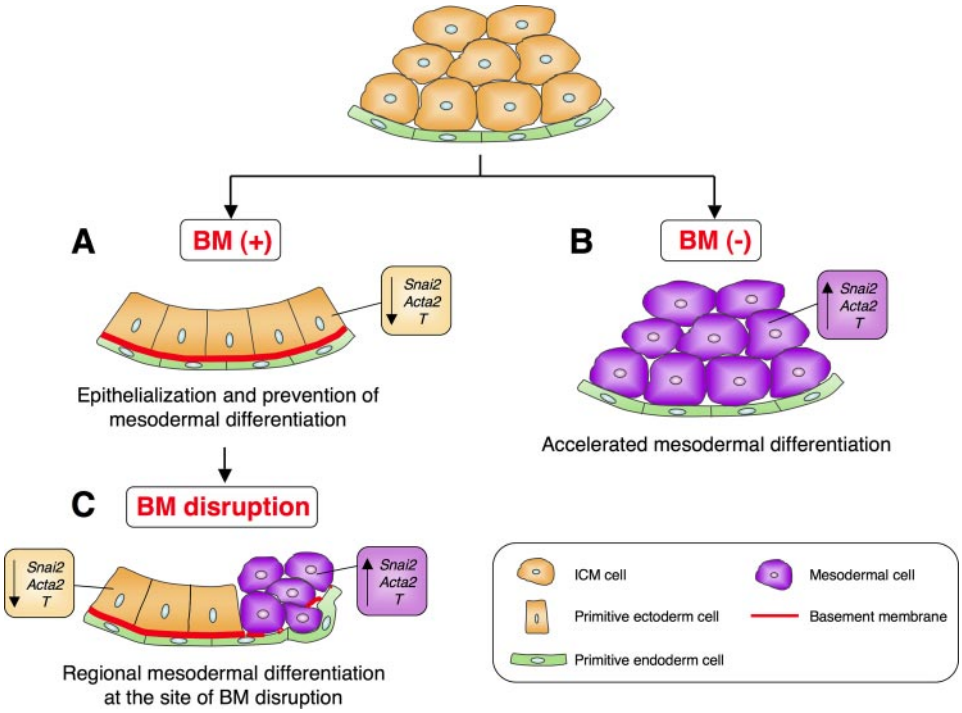

FIGURE 6. **Schematic diagram for BM-dependent control of mesodermal differentiation during EB differentiation.** *A*, deposition of a BM underneath the primitive endoderm not only promotes epithelialization of prospective primitive ectoderm cells adhering to the BM, but also prevents mesodermal differentiation of primitive ectoderm cells by suppressing the expression of EMT-related and mesodermal genes. *B*, in the absence of a BM, the formation of a primitive ectoderm epithelium is inhibited, whereas mesodermal differentiation is not impaired, but rather accelerated. Cells losing contact with the BM cannot resist mesoderm-inducing signals, and are easily converted into mesodermal cells. *C*, at the later stage of normal EB differentiation, the prevention of mesodermal differentiation is lifted when the primitive ectoderm cell-BM interactions are broken by regional disruption of the BM at the time of gastrulation. The initiation of mesodermal differentiation is restricted to the site of BM disruption.

cytoskeleton dynamics essential for EMT initiation are governed by the BM. In the presence of a BM, F-actin accumulated at the apicolateral domain of the polarized primitive ectoderm, which contains cell-cell adhesion machineries. However, in the absence of a BM, F-actin was uniformly distributed around the unpolarized cells and associated with cell-ECM interaction sites, because its distribution overlapped with that of fibronectin. In addition, the cell shape changes induced by rearrangement of the actin cytoskeleton are known to alter the signals generated by cell-ECM interactions and the cellular responses to soluble morphogens (48). Taken together, these observations suggest that the BM orchestrates the dynamics of the actin cytoskeleton and the assembly/disassembly of junctional complexes of epithelial cells, thereby preventing EMT initiation.

Despite the presence of a BM, overexpression of *Snai2* not only induced mesenchymal differentiation, but also inhibited primitive ectoderm epithelialization and cavity formation. These results indicate that BM-induced polarization and cavitation can be overridden by an inhibitory effect of *Snai2* on the initial primitive ectoderm cell polarization. Therefore, the BM appears to induce and maintain the primitive ectoderm epithelialization and cavitation by suppressing the activation of the EMT cascade in the primitive ectoderm. These results also support the possibility that inhibition of apoptosis in the absence of a BM is caused by inhibition of the basal primitive ectoderm epithelialization by activation of the EMT cascade. This possibility is consistent with a previous suggestion by Murray and Edgar that the lack of cavitation in *LAMC1*$^{-/-}$ EBs may result from the absence of polarized primitive ectoderm cells, because the initial stages of cavitation are associated with selective apoptosis of cells positioned at the apical surfaces of the newly formed columnar primitive ectoderm cells (12, 49, 50).

In summary, we have demonstrated a novel BM-dependent mechanism that regulates the mesodermal differentiation of mouse ES cells in EB development. Our data suggest that deposition of a BM beneath the primitive endoderm prevents precocious differentiation of primitive ectoderm toward mesoderm by suppressing the EMT in EBs, which has obvious consequences for the control of mammalian gastrulation. Future studies will need to clarify whether other BM-dependent cell fate determination and differentiation events are also controlled by BM-dependent suppression of the EMT in embryonic development and pathological processes, including cancer progression.

Acknowledgments—We thank Dr. Shaohua Li (Robert Wood Johnson Medical School) for helpful advice on EB formation, Dr. Michael Reth (Max-Planck Institute of Immunology, Germany) for providing the pANMerCreMer vector, and Dr. Mitsuhiro Endoh (RIKEN, Japan) for providing the pCAGGSMerCreMer vector. We express our sincere gratitude to Dr. Nobuo Kato, President of Aichi Medical University, and Dr. Koji Kimata, Director of the Institute for Molecular Science of Medicine, Aichi Medical University, for their enthusiastic encouragement and kind provision of research facilities.

REFERENCES

1. Bissell, M. J., and Labarge, M. A. (2005) *Cancer Cell* **7,** 17–23
2. Hay, E. D. (1991) in *Cell Biology of Extracellular Matrix*, 2nd Ed. (Hay, E. D., ed) pp. 1–6, New York, Plenum Press
3. Gustafsson, E., and Fassler, R. (2000) *Exp. Cell Res.* **261,** 52–68
4. Miner, J. H., Cunningham, J., and Sanes, J. R. (1998) *J. Cell Biol.* **143,** 1713–1723
5. Miner, J. H., and Li, C. (2000) *Dev. Biol.* **217,** 278–289
6. Li, J., Tzu, J., Chen, Y., Zhang, Y. P., Nguyen, N. T., Gao, J., Bradley, M., Keene, D. R., Oro, A. E., Miner, J. H., and Marinkovich, M. P. (2003) *EMBO J.* **22,** 2400–2410
7. Fukumoto, S., Miner, J. H., Ida, H., Fukumoto, E., Yuasa, K., Miyazaki, H., Hoffman, M. P., and Yamada, Y. (2006) *J. Biol. Chem.* **281,** 5008–5016
8. Bader, B. L., Smyth, N., Nedbal, S., Miosge, N., Baranowsky, A., Mokkapati, S., Murshed, M., and Nischt, R. (2005) *Mol. Cell. Biol.* **25,** 6846–6856

9. Nadijcka, M., and Hillman, N. (1974) *J. Embryol. Exp. Morphol.* **32,** 675–695
10. Smyth, N., Vatansever, H. S., Murray, P., Meyer, M., Frie, C., Paulsson, M., and Edgar, D. (1999) *J. Cell Biol.* **144,** 151–160
11. Coucouvanis, E., and Martin, G. R. (1995) *Cell* **83,** 279–287
12. Murray, P., and Edgar, D. (2000) *J. Cell Biol.* **150,** 1215–1221
13. Li, S., Harrison, D., Carbonetto, S., Fassler, R., Smyth, N., Edgar, D., and Yurchenco, P. D. (2002) *J. Cell Biol.* **157,** 1279–1290
14. Viebahn, C. (1995) *Acta Anat.* (*Basel*) **154,** 79–97
15. Viebahn, C., Mayer, B., and Miething, A. (1995) *Acta Anat.* (*Basel*) **154,** 99–110
16. Hayashi, Y., Emoto, T., Futaki, S., and Sekiguchi, K. (2004) *Matrix Biol.* **23,** 47–62
17. Yang, Y. H., Dudoit, S., Luu, P., Lin, D. M., Peng, V., Ngai, J., and Speed, T. P. (2002) *Nucleic Acids Res.* **30,** e15
18. Niwa, H., Yamamura, K., and Miyazaki, J. (1991) *Gene* (*Amst.*) **108,** 193–199
19. Niwa, H., Burdon, T., Chambers, I., and Smith, A. (1998) *Genes Dev.* **12,** 2048–2060
20. Morali, O. G., Delmas, V., Moore, R., Jeanney, C., Thiery, J. P., and Larue, L. (2001) *Oncogene* **20,** 4942–4950
21. Hay, E. D. (1995) *Acta Anat.* (*Basel*) **154,** 8–20
22. Yang, J., Mani, S. A., Donaher, J. L., Ramaswamy, S., Itzykson, R. A., Come, C., Savagner, P., Gitelman, I., Richardson, A., and Weinberg, R. A. (2004) *Cell* **117,** 927–939
23. Barrallo-Gimeno, A., and Nieto, M. A. (2005) *Development* **132,** 3151–3161
24. Verrou, C., Zhang, Y., Zurn, C., Schamel, W. W., and Reth, M. (1999) *Biol. Chem.* **380,** 1435–1438
25. Haub, O., and Goldfarb, M. (1991) *Development* **112,** 397–406
26. Coucouvanis, E., and Martin, G. R. (1999) *Development* **126,** 535–546
27. Jones, C. M., Lyons, K. M., and Hogan, B. L. (1991) *Development* **111,** 531–542
28. Winnier, G., Blessing, M., Labosky, P. A., and Hogan, B. L. (1995) *Genes Dev.* **9,** 2105–2116
29. Xu, C., Inokuma, M. S., Denham, J., Golds, K., Kundu, P., Gold, J. D., and Carpenter, M. K. (2001) *Nat. Biotechnol.* **19,** 971–974
30. Greenlee, A. R., Kronenwetter-Koepel, T. A., Kaiser, S. J., and Liu, K. (2005) *Toxicol. in Vitro* **19,** 389–397
31. Bajanca, F., Luz, M., Raymond, K., Martins, G. G., Sonnenberg, A., Tajbakhsh, S., Buckingham, M., and Thorsteinsdottir, S. (2006) *Development* **133,** 1635–1644
32. Blaess, S., Graus-Porta, D., Belvindrah, R., Radakovits, R., Pons, S., Littlewood-Evans, A., Senften, M., Guo, H., Li, Y., Miner, J. H., Reichardt, L. F., and Muller, U. (2004) *J. Neurosci.* **24,** 3402–3412
33. Georges-Labouesse, E., Messaddeq, N., Yehia, G., Cadalbert, L., Dierich, A., and Le Meur, M. (1996) *Nat. Genet.* **13,** 370–373
34. De Arcangelis, A., Mark, M., Kreidberg, J., Sorokin, L., and Georges-Labouesse, E. (1999) *Development* **126,** 3957–3968
35. Scheele, S., Falk, M., Franzen, A., Ellin, F., Ferletta, M., Lonai, P., Andersson, B., Timpl, R., Forsberg, E., and Ekblom, P. (2005) *Proc. Natl. Acad. Sci. U. S. A.* **102,** 1502–1506
36. Ido, H., Harada, K., Futaki, S., Hayashi, Y., Nishiuchi, R., Natsuka, Y., Li, S., Wada, Y., Combs, A. C., Ervasti, J. M., and Sekiguchi, K. (2004) *J. Biol. Chem.* **279,** 10946–10954
37. Hoffman, M. P., Nomizu, M., Roque, E., Lee, S., Jung, D. W., Yamada, Y., and Kleinman, H. K. (1998) *J. Biol. Chem.* **273,** 28633–28641
38. Talts, J. F., Andac, Z., Gohring, W., Brancaccio, A., and Timpl, R. (1999) *EMBO J.* **18,** 863–870
39. Weir, M. L., Oppizzi, M. L., Henry, M. D., Onishi, A., Campbell, K. P., Bissell, M. J., and Muschler, J. L. (2006) *J. Cell Sci.* **119,** 4047–4058
40. Boucaut, J. C., Darribere, T., Boulekbache, H., and Thiery, J. P. (1984) *Nature* **307,** 364–367
41. George, E. L., Georges-Labouesse, E. N., Patel-King, R. S., Rayburn, H., and Hynes, R. O. (1993) *Development* **119,** 1079–1091
42. Liu, Y. (2004) *J. Am. Soc. Nephrol.* **15,** 1–12
43. Duband, J. L., Monier, F., Delannet, M., and Newgreen, D. (1995) *Acta Anat.* (*Basel*) **154,** 63–78
44. Zeisberg, M., Bonner, G., Maeshima, Y., Colorado, P., Muller, G. A., Strutz, F., and Kalluri, R. (2001) *Am. J. Pathol.* **159,** 1313–1321
45. Savagner, P. (2001) *BioEssays* **23,** 912–923
46. Thiery, J. P., and Sleeman, J. P. (2006) *Nat. Rev. Mol. Cell Biol.* **7,** 131–142
47. Sahai, E., and Marshall, C. J. (2002) *Nat. Rev. Cancer* **2,** 133–142
48. Ingber, D. E. (2002) *Differentiation* **70,** 547–560
49. Murray, P., and Edgar, D. (2001) *Differentiation* **68,** 227–234
50. Murray, P., and Edgar, D. (2004) *Philos. Trans. R. Soc. Lond. B Biol. Sci.* **359,** 1009–1020